Electronic Supplementary Material (ESI) for Nanoscale.

Supplementary information

Ultra-fast stem cell labeling using cationised magnetoferritin

Correia Carreira, S.[a,b], Armstrong, J. P. K.,[c], Seddon, A.M.[a,b], Perriman, A.W.[c], Hartley-Davies[d], R., Schwarzacher, W.[b]

[a] Bristol Centre for Functional Nanomaterials, University of Bristol, Tyndall Avenue, Bristol, BS8 1FD, UK

[b] H.H. Wills Physics Laboratory, University of Bristol, Tyndall Avenue, Bristol, BS8 1TL, UK

[c] School of Cellular and Molecular Medicine, University of Bristol, Medical Sciences Building, University Walk, Bristol, BS8 1TD, UK

[d] Bioengineering, Innovation, and Research Hub, University Hospitals Bristol NHS Foundation Trust, St. Michael's Hospital, Southwell Street, Bristol, BS2 8EG, UK

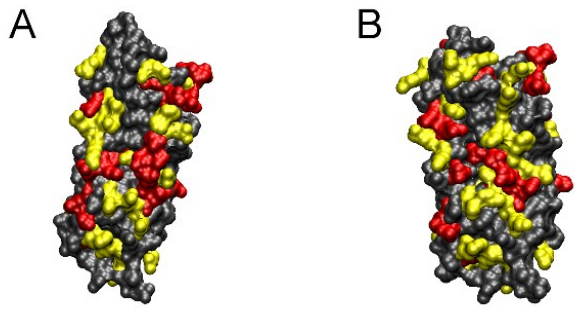

Figure S1. Solvent-accessible surface area representations (1.4 Å probe radius) of mammalian ferritin subunits. Acidic (red), basic (yellow) and neutral (grey) amino acid residues are depicted for (**A**) the light chain (PDB 2W0O) and (**B**) the heavy chain (PDB 2FHA). Number of cationisable sites (aspartate and glutamate residues): 27 on the light chain, 32 on the heavy chain. Horse spleen apoferritin used in this study consists to 90% of the light chain.[1]

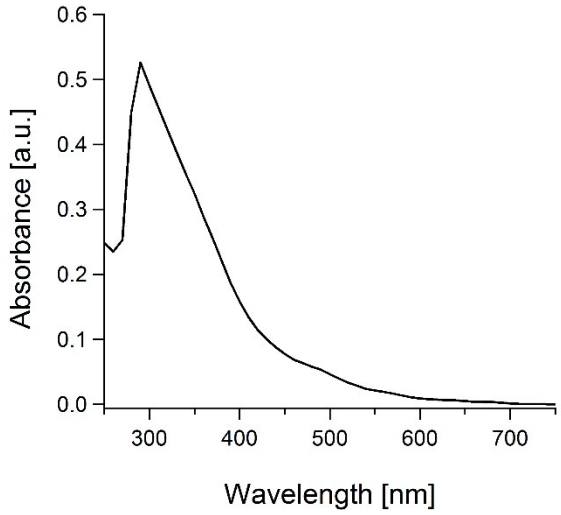

Figure S2. Absorbance spectrum of 1 mg mL^{-1} cat-MF between 250 and 750 nm. Note a shoulder at around 500 nm, which can be attributed to the iron core.[2] Absorbance at 595 nm (wavelength at which Bradford assay is measured) is 0.009.

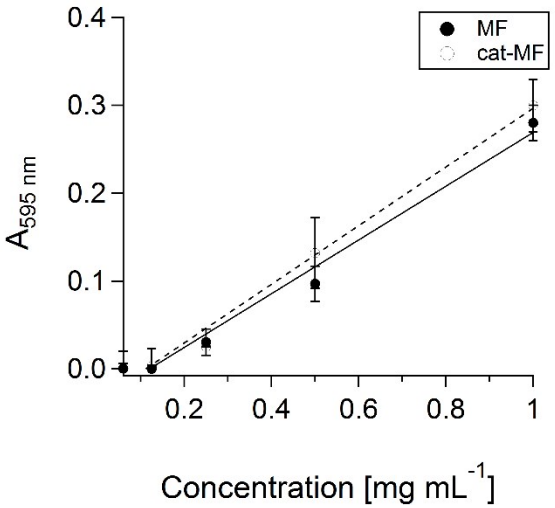

Figure S3. Bradford assay performed on a MF and cat-MF samples of concentrations ranging from 0.06 to 1 mg mL^{-1} (n = 2). The slopes of the linear fit are 0.31 for MF and 0.33 for cat-MF. Absorbance values are similar for MF and cat-MF.

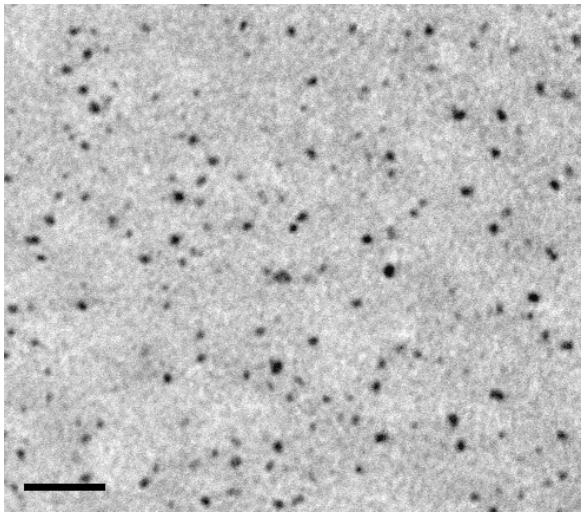

Figure S4. Unstained TEM image of MF used for image analysis of nanoparticle core sizes. Scale bar: 50 nm.

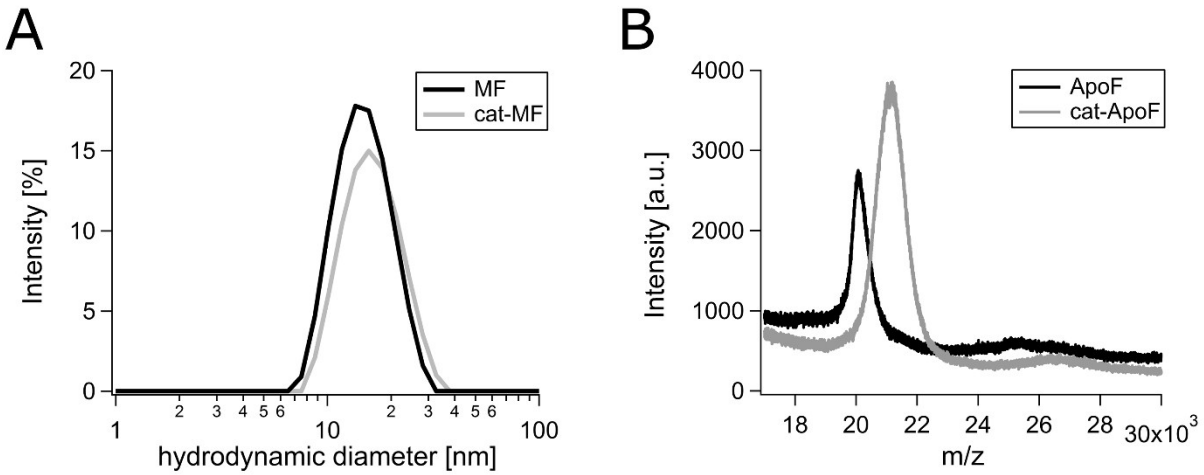

Figure S5. (A) Dynamic light scattering of native magnetoferritin (MF) and cationised magnetoferritin (cat-MF) and (B) matrix assisted laser desorption ionisation time of flight (MALDI-TOF) mass spectroscopy of the native (ApoF) and cationised apoferritin (cat-ApoF) subunit. After cationisation, an increase was observed in both the hydrodynamic diameter and the subunit mass-to-charge ratio (m/z).

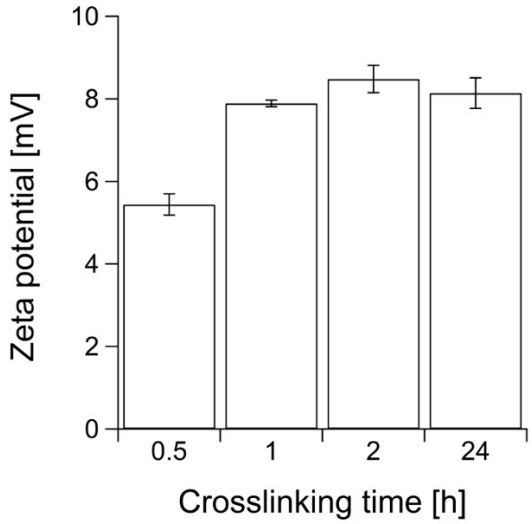

Figure S6. Zeta potential of cationised ferritin prepared using different crosslinking times. The covalent coupling of DMPA using EDC was carried out at pH 5 in all cases.

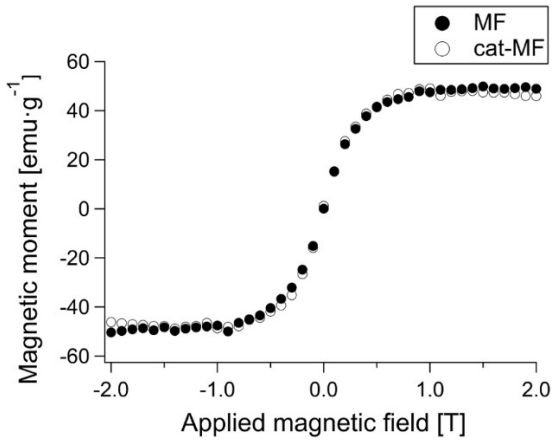

Figure S7. Magnetisation curves of MF and cat-MF at 300 K.

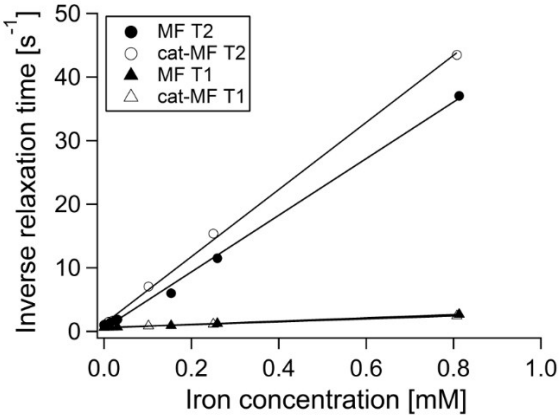

Figure S8. Inverse longitudinal (T1) and transverse (T2) relaxation times of MF and cat-MF plotted as a function of iron concentration. The slope of the linear fit represents the relaxivity (r) of the superparamagnetic core.

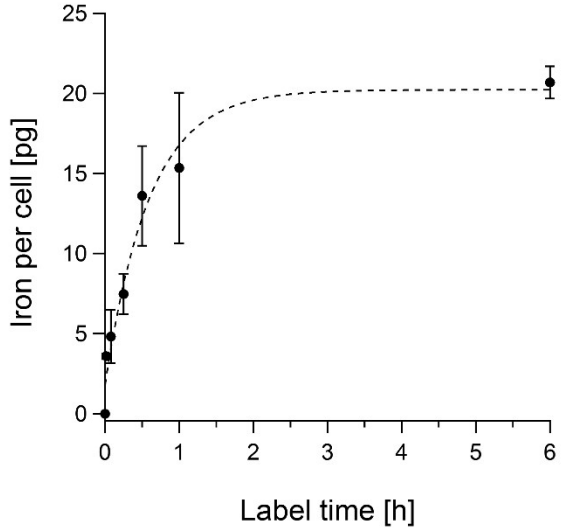

Figure S9. Iron content per cell up to six hours after labelling with 0.5 μM cat-MF. Average and standard deviation of three biological replicates are shown.

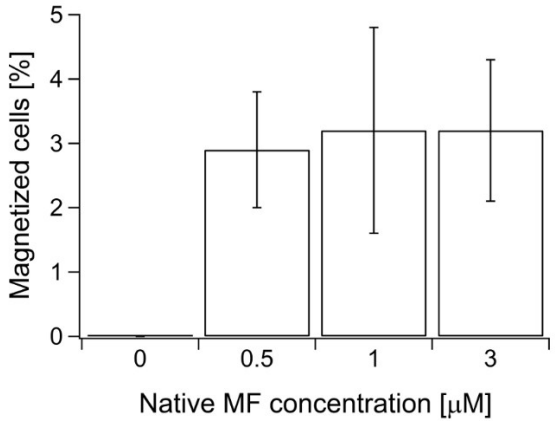

Figure S10. Magnetisation efficiency of cells labeled with various concentrations of MF for 30 minutes. Iron content was below the detection limit of ICP-OES. Average and standard deviation of three biological replicates are shown.

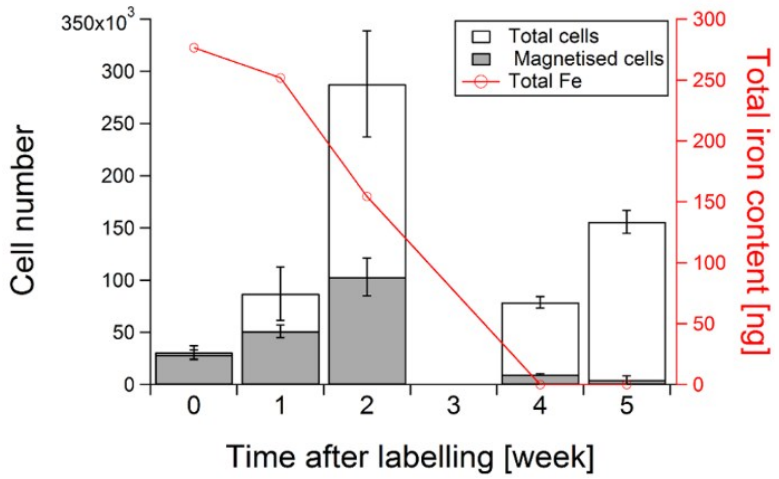

Figure S11. Total cell number, number of magnetised cells and total iron content over 5 weeks in culture after labelling with 0.5 μM cat-MF for 30 minutes. Note that the total cell number appears reduced after 4 weeks, because cells had become confluent and had to be sub-cultured after 3 weeks. For subculturing, the magnetised fraction was separated from the total cells and re-seeded. Average and standard deviation of three biological replicates are shown.

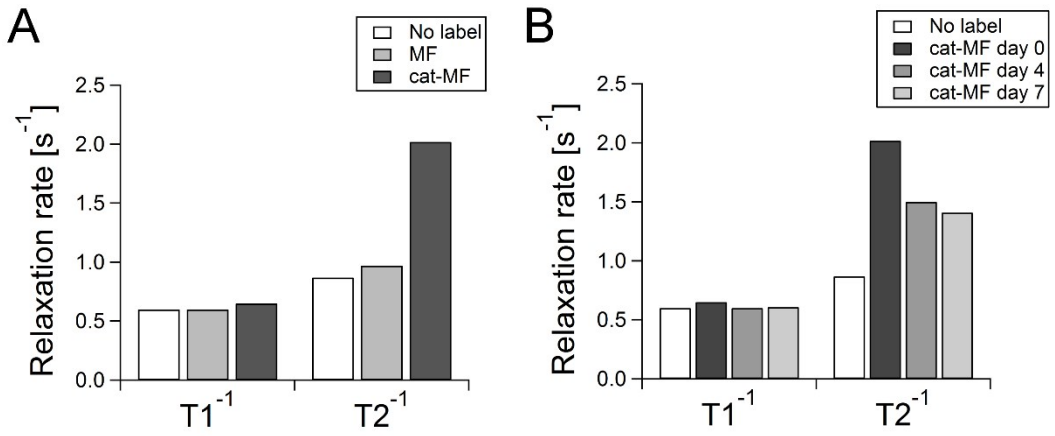

Figure S12. T1 and T2 relaxation rates measured with MRI on 750,000 hMSCs. (A) hMSCs exposed to 0.5 μM of MF and cat-MF for 30 minutes. Little effect on $T1^{-1}$ was observed upon internalisation of MF and cat-MF. Labelling with cat-MF led to a significant increase of $T2^{-1}$, but MF uptake was insufficient to significantly affect $T2^{-1}$ compared to unlabelled cells. (B) MRI of 750,000 hMSCs up to one week after labelling with cat-MF. Little effect on $T1^{-1}$ is observed over time, whilst $T2^{-1}$ is decreased by 30 % after one week.

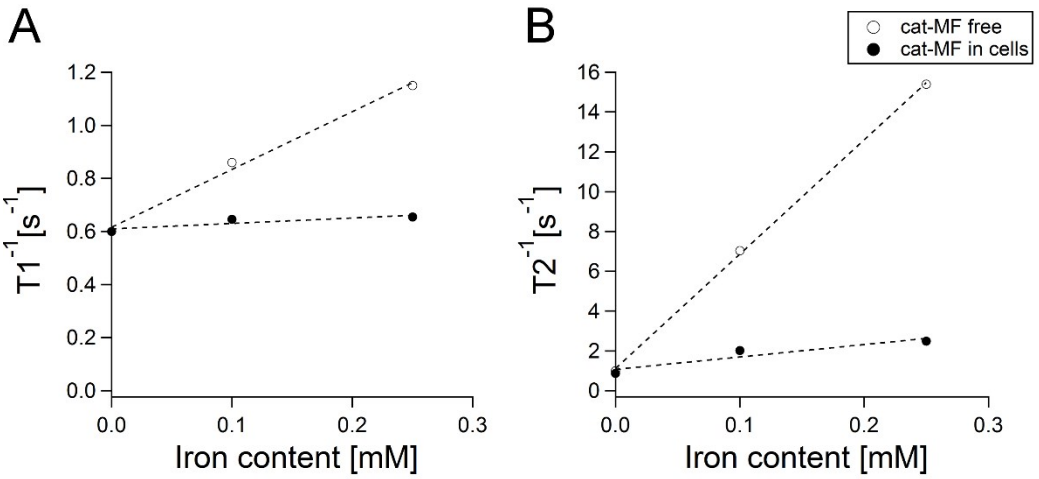

Figure S13. Effect of cellular internalisation of cat-MF on relaxation rates. (A) The longitudinal (r1) and (B) the transverse relaxation rate (r2) as a function of iron content measured in the samples of hMSCs exposed to 0.5 and 1 μM cat-MF. The dashed line is the linear fit to the experimental data and represents the molar relaxivity values: $r1_{free}$: 2.6 $mM^{-1}s^{-}1$; $r1_{cell}$: 0.2 $mM^{-1}s^{-}1$; $r2_{free}$: 52.8 $mM^{-1}s^{-1}$; $r2_{cell}$: 7.7 $mM^{-1}s^{-1}$

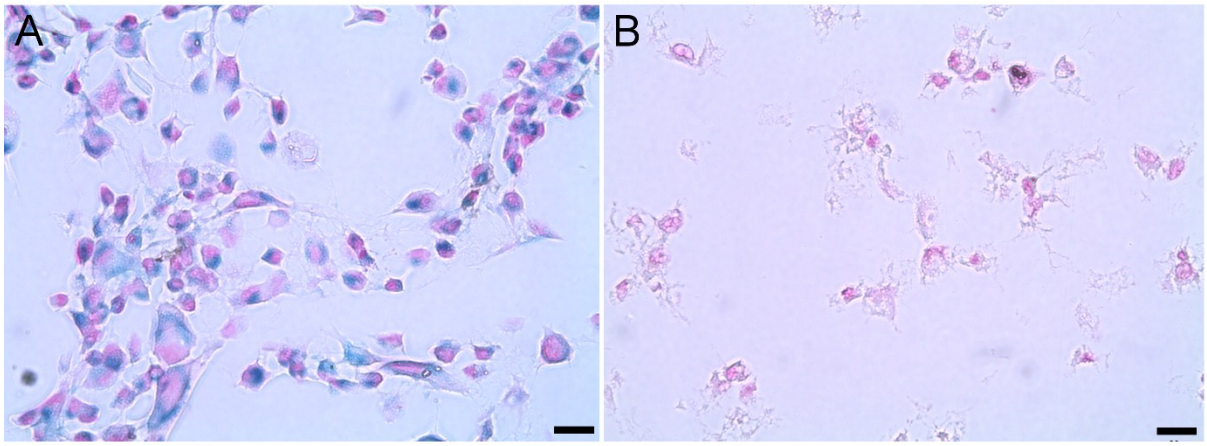

Figure S14. Prussian Blue staining of sectioned hMSCs (A) 48 hours after exposure to cat-MF. Cells were exposed to 0.5 μM cat-MF for 30 minutes in 75 cm2 flasks and left to incubate for 24 hours. After that, they were seeded onto fibronectin-coated PGA scaffolds and left to adhere to the scaffold over night. Scaffolds were fixed in paraformaldehyde, embedded in paraffin wax and sectioned. The blue stain is localised inside the cells and indicates that cat-MF has been internalised. Cell nuclei were counter-stained with Nuclear Fast Red and appear pink. (B) Untreated control. No blue stain is visible inside the cells. All scale bars: 20 μm.

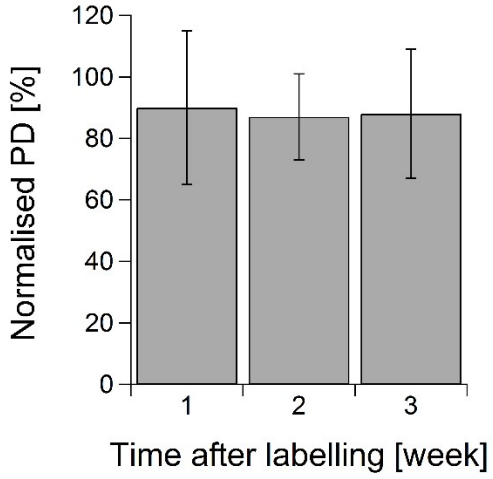

Figure S15. Proliferation of hMSCs was determined with a weekly cell counting assay after exposure to 0.5 μM cat-MF for 30 minutes, and found to be similar to proliferation of untreated cells. PD: Population doublings.

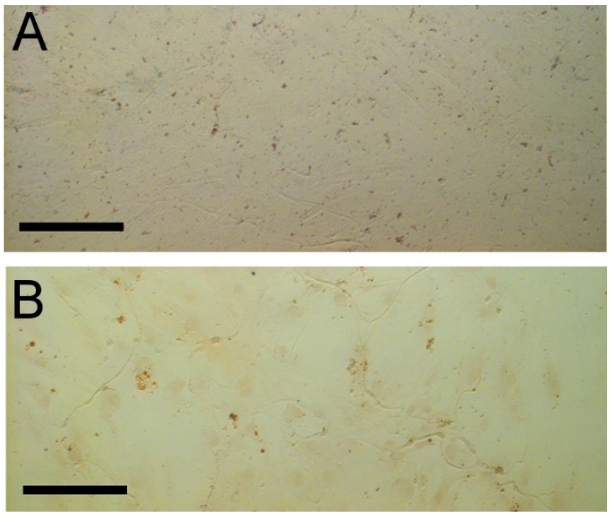

Figure S16. Bright field microscopy images of hMSCs labeled with 1 μM cat-MF for 30 minutes after three weeks in culture. (**A**) Undifferentiated hMSCs stained with Oil Red showing no visible fatty vacuoles. (**B**) Undifferentiated hMSCs stained with Alizarin Red showing no visible calcium phosphate deposits. All scale bars: 100 μm.

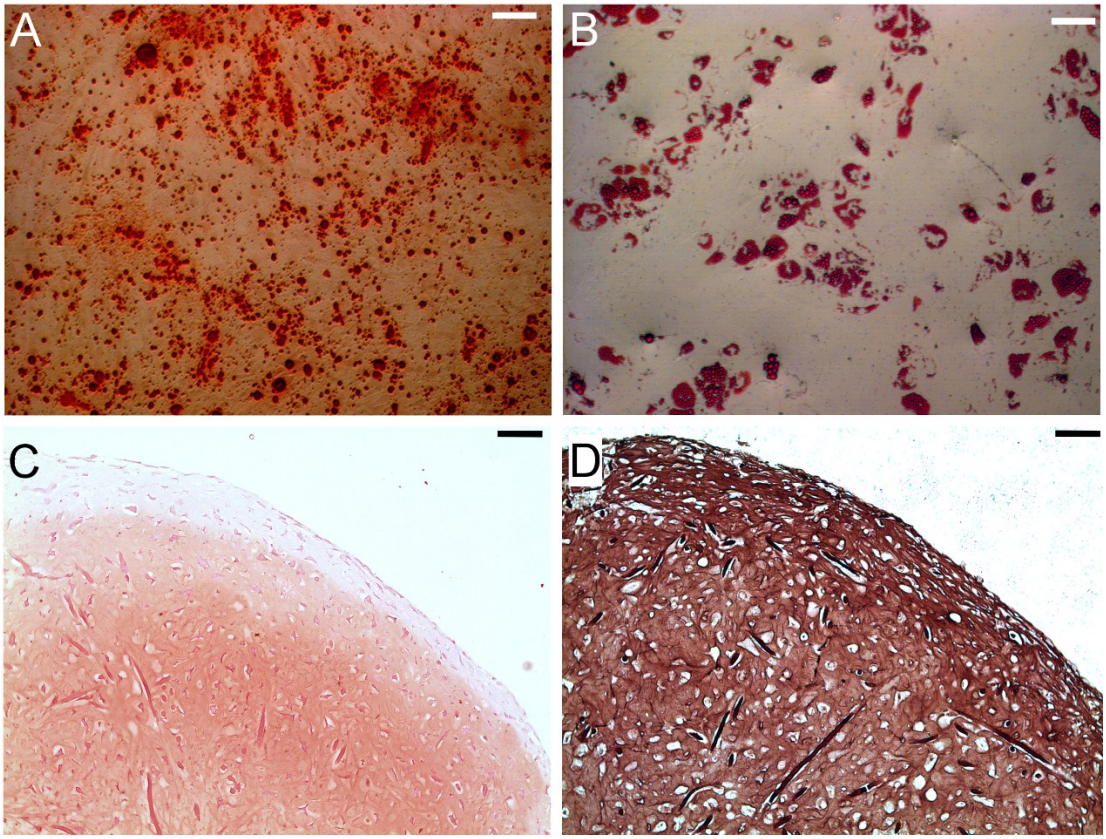

Figure S17. Differentiation capacity of untreated hMSCs. Representative bright field microscopy images of (A) hMSC-derived osteoblasts with calcium phosphate deposits stained with Alizarin Red. (B) hMSC-derived adipocytes with fatty vacuoles stained using Oil Red. (C) Section of engineered cartilage tissue construct stained for proteoglycans with Safranin O and (D) stained for collagen type II using an immunohistochemical staining procedure. All scale bars: 100 μm.

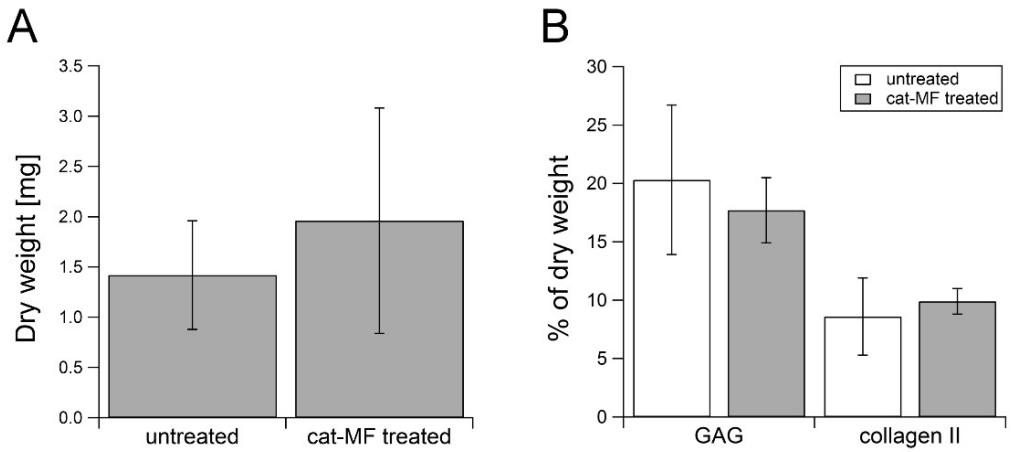

Figure S18. Biochemical analysis of cartilage tissue constructs. (A) The dry weights of engineered cartilage tissue constructs derived from untreated hMSCs and hMCSc treated with 0.5 μM cat-MF. Average and standard deviation of three biological replicates are shown. (B) Quantification of glycosaminoglycans (GAG) and collagen type II extracted from the dried cartilage tissue constructs. Average and standard deviation of three biological replicates are shown (with exception of the cat-MF treated collagen II value, which was determined from extracts of two cat-MF treated cartilage constructs due to insufficient sample volume to conduct the assay).

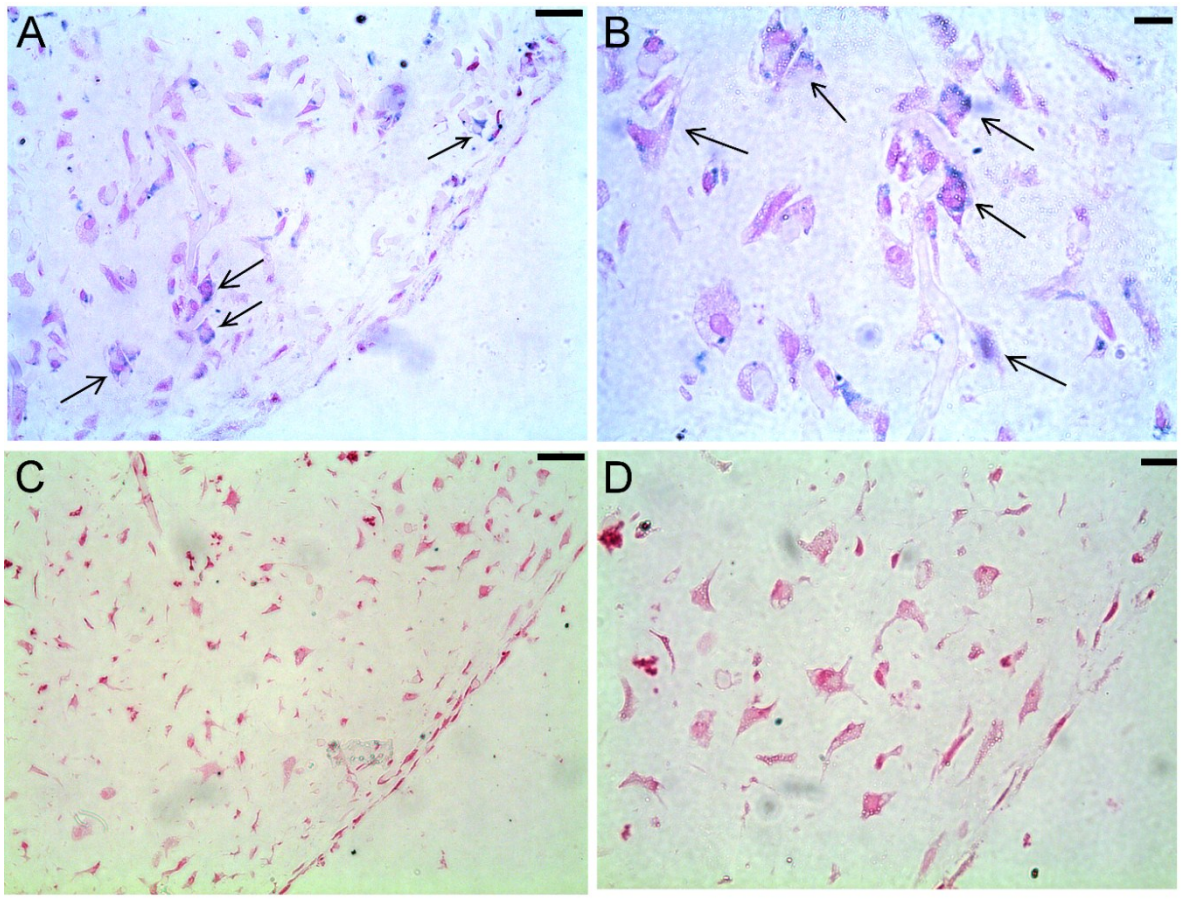

Figure S19. Prussian Blue staining of cartilage tissue constructs. Representative bright field microscopy images of (A, B) histological sections of cartilage constructs derived from cat-MF labelled hMSCs. The blue stain indicates iron deposits. Cell nuclei were counter-stained with Nuclear Fast Red and appear pink. (C, D) histological sections of cartilage constructs derived from untreated hMSCs. No blue stain is visible. Sections were imaged using a (A, C) 20x objective, scale bar 50 μm and (B, D) 40x objective, scale bar 20 μm.

References:

1. Stefanini, S.; Chiancone, E.; Arosio, P.; Finazziagro, A.; Antonini, E. Structural Heterogeneity and Subunit Composition of Horse Ferritins. *Biochemistry* **1982**, *21*, 2293-2299.

2. Koralewski, M.; Pochylski, M.; Gierszewski, J. Magnetic properties of ferritin and akaganeite nanoparticles in aqueous suspension. *J Nanopart Res* **2013**, *15*, 1902-1922.